Long-Range Diffusion in Xylitol-Water Mixtures

ARTICLE *in* THE JOURNAL OF PHYSICAL CHEMISTRY B · MAY 2013

Impact Factor: 3.3 · DOI: 10.1021/jp401633g · Source: PubMed

5 AUTHORS, INCLUDING:

Khalid Hassan Elhadi Elamin
Chalmers University of Technology
8 PUBLICATIONS **33** CITATIONS
SEE PROFILE

Johan Sjostrom
SP Technical Research Institute of Sweden
29 PUBLICATIONS **212** CITATIONS
SEE PROFILE

Stephen Michael King
Science and Technology Facilities Council
141 PUBLICATIONS **2,117** CITATIONS
SEE PROFILE

Jan Swenson
Chalmers University of Technology
177 PUBLICATIONS **3,992** CITATIONS
SEE PROFILE

THE JOURNAL OF PHYSICAL CHEMISTRY B

Article

pubs.acs.org/JPCB

Long-Range Diffusion in Xylitol–Water Mixtures

Khalid Elamin,[†] Stefano Cazzato,[†] Johan Sjöström,[‡] Stephen M. King,[§] and Jan Swenson*,[†]

[†]Department of Applied Physics, Chalmers University of Technology, SE-412 96 Göteborg, Sweden

[‡]SP Technical Research Institute of Sweden, SE-501 15 Borås, Sweden

[§]ISIS Facility, Rutherford Appleton Laboratory, Chilton, Didcot, OX11 0QX Oxfordshire, United Kingdom

ABSTRACT: Dynamic light scattering (DLS) and small-angle neutron scattering (SANS) were employed to study mixtures of xylitol and water. The results were also related to a previous dielectric relaxation study on the same system. In the temperature range of the DLS measurements the viscosity related structural (α) relaxation is too fast to be observed on the experimental time scale, but a considerably slower exponential and hydrodynamic relaxation process is clearly observable in the polarized light scattering data. A similar ultraslow process has been observed in many other types of binary liquids and commonly assigned to long-range concentration or density fluctuations. In some studies this interpretation has been supported by observations of substantial structural inhomogeneities in static light scattering or SANS experiments. However, in this study we observe such an ultraslow process without any indication of structural inhomogeneities on length-scales above 2 nm. Hence, we suggest that our observed ultraslow process is due to long-range diffusion of single xylitol molecules or small clusters of a few xylitol molecules (and perhaps some associated water molecules) which are randomly dispersed and sufficiently small to not be structurally detected in our SANS study. In the q-range of the DLS measurements this ultraslow relaxation process is around room temperature several orders of magnitude slower than the structural α-relaxation. However, if its $1/q^2$-dependent relaxation time is extrapolated to q-values where relaxation times from dielectric spectroscopy and quasielastic neutron scattering are compatible (about 10 nm^{-1}), a relaxation time similar to that of the dielectric α-relaxation is obtained. Thus, the large difference in time scale between the two relaxation processes in the q-range of a DLS study is due to the fact that the α-relaxation is cooperative in nature, rather than caused by long-range single particle diffusion, and thus q-independent at low q-values.

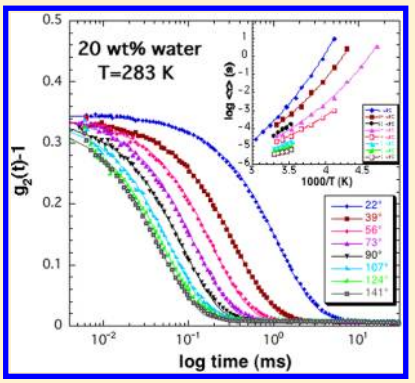

1. INTRODUCTION

The liquid state cannot be fully understood without understanding the microscopic dynamics of liquids, which determine many of their macroscopic properties. For instance, many types of liquids have been found to exhibit a poorly understood ultraslow relaxation process, i.e., a process that is slower than the viscosity related structural (α) relaxation. Such a process has been observed in many glass-forming liquids by a wide range of different experimental techniques, such as dynamic light scattering (DLS),[1−4] dielectric spectroscopy,[5−9] and brillouin ultraviolet scattering,[10] and is generally acknowledged to be caused by long-range density fluctuations[11] or concentration fluctuations in the case of binary liquids.[12] However, despite the fact that the ultraslow DLS process has been investigated in detail,[13−18] the physical nature and the possible universality of it are still not fully established. Different scenarios have been proposed from the experimental data to understand the structure, kinetics, and dynamics related to the relaxation process. For instance, in ref 1 aqueous glucose solutions were studied by static and dynamic light scattering, and an ultraslow process could be observed in the polarized dynamic scattering data. Sidebottom[1] attributed this ultraslow process to the diffusion of hydrogen bonded clusters of glucose molecules in the solutions. From the static light scattering data the size of the clusters was determined to be in the range between 30 and 60 nm, depending on the water concentration. However, a more recent estimation of the cluster size from the DLS data indicated a much larger concentration dependence of the cluster size.[3] In this latter study it was found, by applying the Stokes–Einstein relation with the viscosity of water for the diffusing sugar clusters, that the hydrodynamic radius of the clusters increased in a power law fashion, extrapolating to infinitely large clusters at a weight fraction of 82.5 wt % sugar.[3] Thus, at high water concentrations the diffusing particles were found to be single sugar molecules, but at low water concentrations the size of the particles increased rapidly with decreasing water content.[3] However, it should be noted that if the calculation of the hydrodynamic radius was based on the macroscopic viscosities of the solutions, instead of the viscosity of water, no cluster formation would be obtained for any sugar concentration.

In ref 1 it was also found that in contrast to the faster α-relaxation, which was observed in both polarized and depolarized scattering data, the ultraslow process exhibited an exponential relaxation behavior with a strong wave vector (q) dependence, as is typical for hydrodynamic relaxation

Received: February 15, 2013
Revised: May 22, 2013
Published: May 23, 2013

   dx.doi.org/10.1021/jp401633g | J. Phys. Chem. B 2013, 117, 7363−7369

processes. Support to the interpretation that the ultraslow process observed in ref 1 is due to the diffusion of clusters comes also from a dynamic light scattering study of orthoterphenyl (OTP, also known as diphenylbenzene) by Patkowiski et al.[2] The authors formed two types of OTP structures, with and without clusters, and it was found that only the structure containing clusters exhibited the same type of ultraslow process as observed for aqueous glucose solutions.[1] Further support that this type of ultraslow process is due to a collective diffusive motion of a large number of molecules is that its temperature dependence can be described by the same type of Vogel–Fulcher–Tammann (VFT) function[19−21] as used for the α-relaxation, with the same fit parameters B and T_0, but with a much larger value of τ_0. The large value of τ_0 is a direct indication that the process is of collective nature with an involvement of a large number of molecules in the relaxation process.

Also in dielectric relaxation studies a similar ultraslow process has been observed. In dielectric spectroscopy the ultraslow process is identified by a low-frequency Debye peak in the imaginary part of the permittivity (the Debye shape is unusual for amorphous materials, which generally exhibit broader relaxation processes). This Debye peak is most pronounced for monoalcohols, where it is considerably stronger than the viscosity related α-relaxation, but it has also been observed in polyalcohols and their mixtures,[5−7] as well as in other types of hydrogen bonded molecular systems.[8,9] However, whether the physical origin of the Debye peak is the same for all these types of materials and whether it is directly related to the ultraslow process probed in dynamic light scattering experiments is far from established. In fact, from recent studies of monoalcohols[22,23] it seems unlikely that the dielectrically observed Debye peak can be related to the same type of cluster motions as observed with dynamic light scattering. Thus, despite the similarities in the observed features of the ultraslow process, its physical origin might be strongly dependent on the material.

In this paper we have elucidated the possibility of ultraslow dynamics in xylitol–water mixtures by dynamic light scattering (photon correlation spectroscopy) and compared our findings with our recently published[24] dielectric relaxation data. In ref 24 our main aim was to elucidate whether we should find the same behavior for water–xylitol solutions as other scientists have observed for the similar water–glycerol system. From that study we could conclude that we observed the same calorimetric behavior as for the water–glycerol system,[25] but we found no clear indication from our dielectric studies that concentration fluctuations occur at higher water contents, as was proposed for the water–glycerol system.[26] Therefore, the aim of this study was mainly to elucidate the possibility of concentration fluctuations in more detail.

The results from the present DLS measurements show, indeed, the presence of an ultraslow relaxation process, but from our complementary small-angle neutron scattering (SANS) experiments we find no evidence for any significant excess scattering from any of the solutions in the momentum transfer (q) range corresponding to length-scales from about 2 to 100 nm. Thus, despite the fact that the DLS measurements show a slow process, exhibiting a $1/q^2$-dependent relaxation time, as typical for long-range diffusion, we fail to detect any significant structural inhomogeneities in the SANS measurements. From the diffusion constant we have tried to estimate the size of the diffusing particles by using the Stokes–Einstein relation. However, as discussed below, this is a difficult task due to the fact that it is not obvious what the relevant "microscopic viscosity" should be for the calculations. By using the macroscopic viscosity of each mixture the particle size becomes unrealistically small, i.e., smaller than the size of a xylitol molecule, at least at low water concentrations. Alternatively, by using the viscosity of water for all mixtures, the value of the "microscopic viscosity" is likely underestimated, particularly at low water concentrations and low temperatures, and consequently the size of the diffusing particles becomes overestimated. Nevertheless, this latter approach gives an upper limit of the particle size and indicates that not more than a few xylitol molecules can move together as a diffusing particle.

2. SAMPLE PREPARATIONS AND EXPERIMENTAL METHODS

2.1. Dynamic Light Scattering. We have investigated mixtures of xylitol ($C_5H_{12}O_5$) (≥99% purity, purchased from Sigma, C.A.S number (87-99-0)) and double distilled water (Milli-Q water) over a broad concentration range from 9 wt % (40 mol %) up to 80 wt % (96 mol %) water. The solutions with less than 50 wt % (87 mol %) water were produced by first mixing equal weights of xylitol and distilled water in an ultrasonic bath. This solution was thereafter filtered to remove any dust particles, before it was poured into sample cells. The final water content of the solution was obtained by keeping the 50 wt % water solution of an oven at a temperature of 353 K until the desired amount of water had been evaporated. The samples with more than 50 wt % water were prepared in the same way, except that the amounts of xylitol and distilled water were chosen to directly give the desired composition of the solution.

Two different dynamic light scattering (DLS) setups were used for the present study, depending on the temperature of the measurements. For those samples demanding a study of the dynamics at temperatures lower than 280 K, a DLS apparatus was used where the sample cell was mounted in an Oxford continuous flow cryostat (CF1204). The sample was illuminated by a 150 mW 532 nm focused laser beam from a compact diode-pumped solid-state Oxxius single mode source. Scattered light was collected in 90° polarized scattering geometry, coupled into a single mode optical fiber, and fed through a beam splitter into two fast photomultipliers operating in a pseudo-cross-correlation mode.

For measurements in the temperature range between 280 and 328 K an ALV/CGS-8F light scattering instrument was used. This instrument is equipped with a laser source of the same kind as described above, and eight photomultiplier detectors, working in normal autocorrelation mode and at different scattering angles. Here, the sample environment is constituted by the usual index-matching vat filled with toluene—whose temperature is controlled by means of a thermal bath—to reduce spurious scattering from the walls of the sample vial.

Hardware ALV-7400/FAST Multiple Tau digital correlators were utilized by both setups, providing up to 288 correlation channels with an initial lag time of 25 ns. The DLS data of each sample were collected at different temperatures, typically for 2 h at each temperature, after waiting at least 30 min for thermal equilibration. The output of the correlator is the normalized count rate (intensity) autocorrelation function $g_2(t) = \langle I(0)I(t)\rangle/\langle I\rangle^2$, which, in the present case of homodyne detection, is related to the normalized electric field autocorrelation function $g_1(t)$ through $g_2(t) = 1 + ag_1^2\langle t\rangle$, where $a \leq 1$ is an instrumental

dx.doi.org/10.1021/jp401633g | J. Phys. Chem. B 2013, 117, 7363−7369

coherence factor,[27] related to the number of simultaneously detected coherence areas[27] and, in the case of single mode fiber light collection, is expected to be about 1. We measured a using a polystyrene latex standard and found that $a = 0.994 \pm 0.001$.

2.2. Small-Angle Neutron Scattering. The SANS measurements were performed on the instrument SANS2D at the pulsed neutron spallation source ISIS at the Rutherford Appleton Laboratory, U.K.[28,29] SANS2D is a "white beam" time-of-flight instrument, which utilizes neutrons with wavelengths, λ, between 0.2 and 1.4 nm. Data are simultaneously recorded on two, moveable, two-dimensional position-sensitive neutron detectors, to provide a maximum q-range of 0.02−30 nm^{-1}. The same xylitol as used for the DLS measurements was also used for the SANS measurements, however, the distilled H_2O was replaced by D_2O in order to enhance the neutron scattering contrast between xylitol and water. It should here be noted that the actual contrast in scattering from water and xylitol was reduced by the rapid and continuous H−D exchange between the H-atoms of the OH groups on xylitol and the D-atoms of D_2O. Nevertheless, small-angle scattering would still be expected in the case of an inhomogeneous mixture of the two liquids. However, to improve measurement statistics, a high count-rate configuration of the instrument was utilized (1 mm path length quartz cuvettes, 12 mm beam diameter, and a sample-to-detector distance of 3.0 m). With this setup a q-range of 0.06−11 nm^{-1} was obtained, sufficient to observe concentration fluctuations on an experimental length scale of about 0.6 to 100 nm if present. Each sample and background was measured for about 3 h in order to gather data of high statistical precision. Each raw scattering data set was corrected for the detector efficiencies, sample transmission, and background scattering and converted to scattering cross-section data ($\partial\Sigma/\partial\Omega$ vs q) using the software package Mantid.[30]

3. EXPERIMENTAL RESULTS

In Figure 1 the intensity−intensity autocorrelation function ($g_2(t) - 1$) is shown for different scattering angles and temperatures. Figure 1a shows the angular dependence of the autocorrelation function for a xylitol−water solution with 20 wt % (63 mol %) water at $T = 283$ K. The data were obtained on the ALV/CGS-8F light scattering instrument, where all scattering angles were measured simultaneously. The statistics are excellent, and it is evident from the data that only one single exponential relaxation process can be observed in the experimental time window. In Figure 1b data are shown for a solution with 35 wt % (78 mol %) water in the temperature range 243−300 K at a scattering angle of 90°. These data were obtained with the other spectrometer, using the Oxford coldfinger cryostat, where lower temperatures can be reached, but only one scattering angle is covered at each measurement. From the data shown in Figure 1b it is also clear that the statistical errors become substantially larger with this experimental setup. The inset of Figure 1b shows how the amplitude of $g_2(t) - 1$ changes with the concentration of water in the solution. The results indicate that the scattering contrast increases with increasing water content, up to at least 80 wt % water.

The physical nature of the observed relaxation process can be elucidated by investigating its q-dependence. This has been done in Figure 2, which shows how the relaxation time τ depends on $1/q^2$ for different compositions at $T = 288$ K in (a) and at different temperatures for the solution with 40 wt % (82 mol %) water in (b). For all samples and temperatures the data

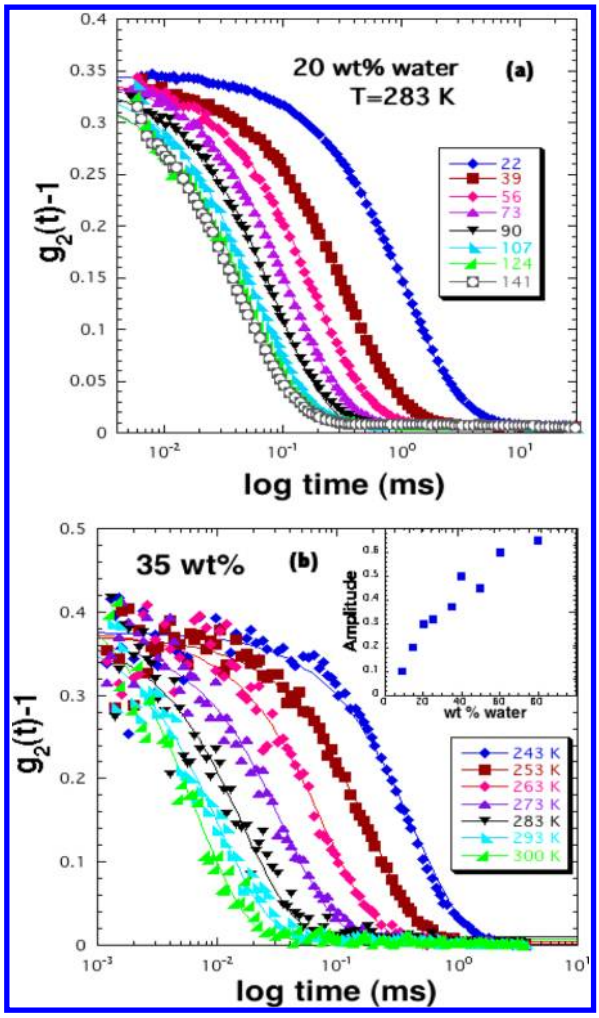

Figure 1. Intensity−intensity autocorrelation function $g_2(t) - 1$ for (a) a xylitol−water solution with 20 wt % water at different scattering angles (θ) and $T = 283$ K and (b) a xylitol−-water solution with 35 wt % water in the temperature range 243−300 K at a scattering angle of 90°. The solid lines are single exponential fits to the data. The inset in (b) shows the amplitude of $g_2(t) - 1$ as a function of the water content in the solution.

are well described by lines of slope of 1 in the shown log−log presentation, which imply a linear relation, i.e., that τ is proportional to $1/q^2$, as expected for long-range translational diffusion.

In Figure 3 relaxation times of the observed DLS process, as well as previously obtained[24] dielectric relaxation times for the α-process, are plotted as a function of the inverse temperature. The relaxation times from the DLS measurements were obtained for 90° scattering angle, corresponding to a q-value of about 0.025 nm^{-1}. In the figure it is evident that both processes are strongly concentration dependent and exhibit non-Arrhenius temperature dependences. The DLS process is considerably slower at high temperatures, and due to its weaker temperature dependence, this process extrapolates to about 100 s at the calorimetric T_g of the sample. The glass transition temperatures of the xylitol−water solutions can be estimated calorimetrically,[24] from differential scanning calorimetry (DSC) measurements, as well as dynamically, from both dielectric spectroscopy[24] and dynamic light scattering, as the temperature where the viscosity related α-relaxation and, here, the observed DLS relaxation, respectively, reach a relaxation time of 100 s

dx.doi.org/10.1021/jp401633g | J. Phys. Chem. B 2013, 117, 7363−7369

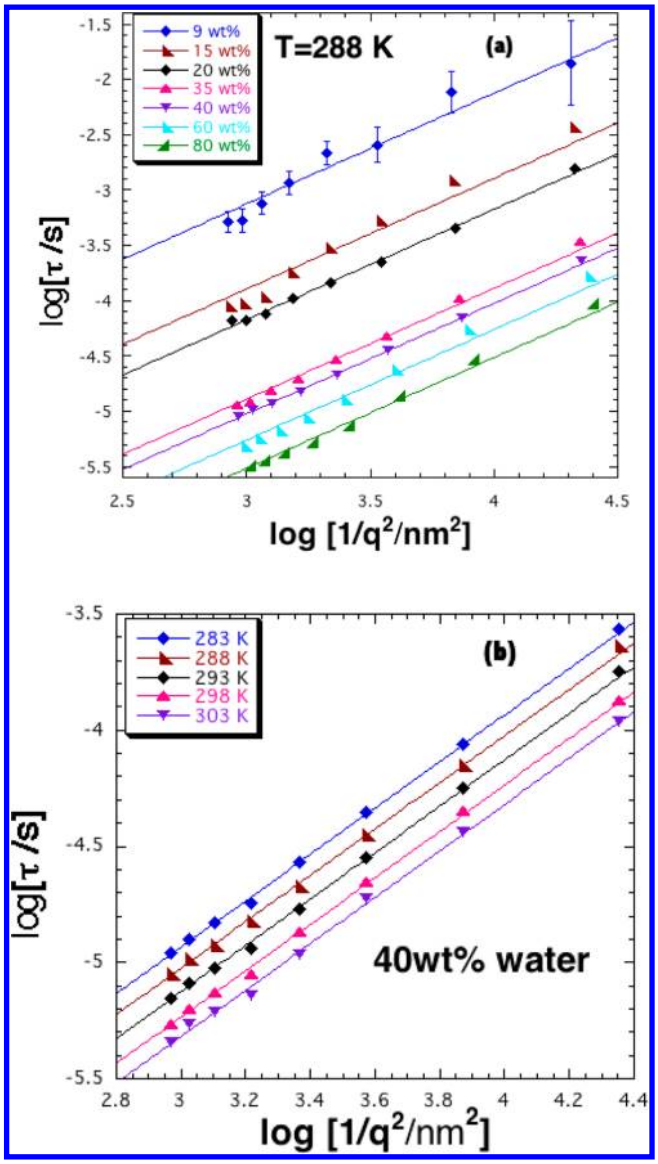

Figure 2. Dependence of relaxation time on $1/q^2$ for (a) different compositions at T = 288 K and (b) at different temperatures for the solution with 40 wt %. The lines have a slope of 1 and show that τ is proportional to $1/q^2$, as expected for long-range translational diffusion. The τ-values were obtained from exponential fits to the experimental $g_2(t) - 1$ data, as shown in Figure 1.

(Figure 4). However, it should be noted that the temperature dependences of the relaxation times obtained from the DLS measurements on the solutions of high water contents need to be extensively extrapolated in order to reach relaxation times of 100 s, i.e., the error bars of these estimated T_g are large. Furthermore, the extrapolations of the water rich solutions must be regarded as artificial, since substantial ice formation would occur in reality in the deeply supercooled regime. It is also questionable whether the Gordon−Taylor equation can be used to estimate the T_g of bulk water and water rich solutions since it is likely that the structural and dynamical properties of water are strongly dependent on the water concentration of the solution.[31] Thus, the meaning of the extrapolations at high water contents, and the so obtained T_g-values, is questionable, but it is an interesting observation that the DLS relaxation exhibits a dynamic glass transition at the same temperature as the viscosity related α-relaxation.

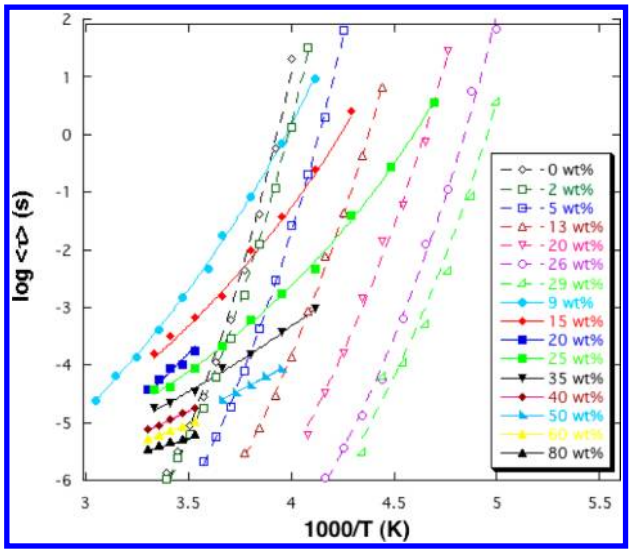

Figure 3. Temperature dependences of relaxation times obtained from exponential fits to the experimental $g_2(t) - 1$ data taken at 90° scattering angle, which corresponds to a q-value of about 0.025 nm^{-1}. Previously obtained[24] dielectric relaxation times for the viscosity related α-process are also shown for comparison. Solid symbols correspond to DLS data and open symbols to dielectric relaxation data.

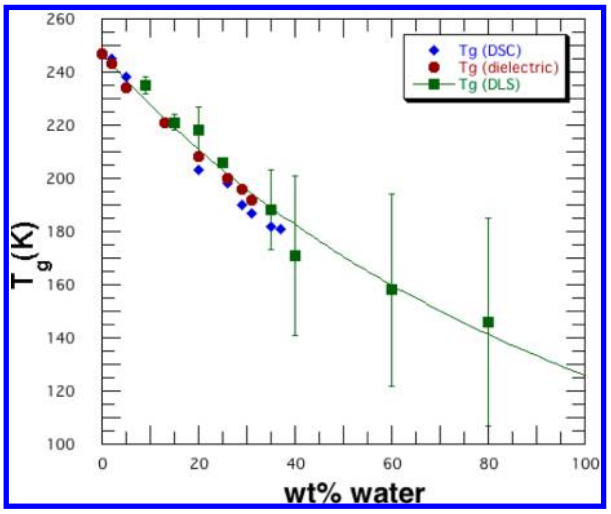

Figure 4. Concentration dependence of the estimated temperature where the observed DLS relaxation reaches a relaxation time of 100 s. From the figure it is evident that this "freezing-in" of the DLS relaxation occurs at the same temperature as the calorimetric glass transition from DSC measurements,[24] as well as the dynamic glass transition from dielectric spectroscopy,[24] estimated as the temperature where the viscosity related α-relaxation reaches a time scale of 100 s. The concentration dependence of T_g is described by a Gordon−Taylor fit (solid line).

Figure 5 shows the differential neutron scattering cross-section at T = 295 K for xylitol−water mixtures containing 20, 40, 60, and 80 wt % (63, 82, 91, and 96 mol %) heavy water. The momentum transfer (= scattering vector, q) axis has been truncated to emphasize the data at low q values. Corresponding data for pure H_2O and pure D_2O are also shown for comparison. A small increase of the scattering is observed at the lowest q-values for the samples with ≥40 wt % xylitol. However, this is a common feature of hydrogen containing samples and therefore is clearly observed also for pure H_2O. It is considered to be caused by inelasticity effects in the

dx.doi.org/10.1021/jp401633g | J. Phys. Chem. B 2013, 117, 7363−7369

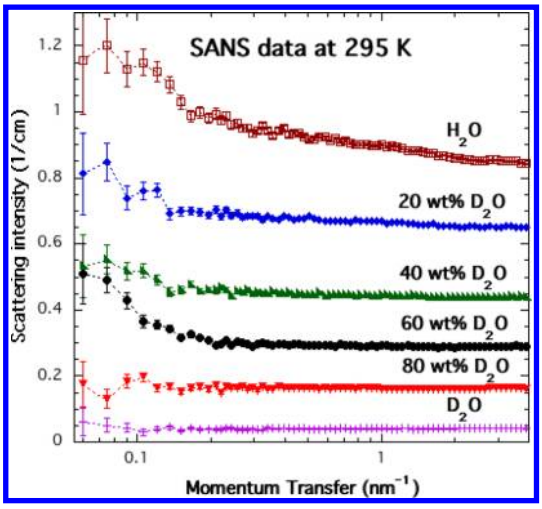

Figure 5. Differential coherent neutron scattering cross section at T = 295 K for xylitol−water mixtures containing 20, 40, 60, and 80 wt % water and for pure H_2O and pure D_2O, for comparison. The scattering contributions from the quartz cuvettes have been subtracted from the measured data. The dotted lines are a guide for the eye.

scattering from light hydrogen atoms. Unfortunately, there is no method to safely correct the data for such effects. However, the important observation is that the q-dependent scattering from the solutions is very much the same as might be expected from homogeneous mixtures of H_2O and D_2O with the same volume fractions of hydrogen. Thus, none of the solutions show obvious evidence of any significant scattering in excess of that from homogeneous liquids having the same incoherent scattering cross sections. Since the scattering cross section is directly proportional to the product of the volume fraction of any scattering entities present multiplied by the volume of one scattering entity, this observation is a clear indication of the absence of any xylitol clusters at length scales in the range 2−100 nm (corresponding to the shown q range 0.06−4 nm^{-1}).

4. DISCUSSION

A single exponential character of the relaxation function, an ultraslow relaxation time, i.e., considerably slower than the viscosity related α-relaxation, at high temperatures, and, in particular, a $1/q^2$ dependence of the relaxation time are all features of a previously observed relaxation process interpreted as caused by concentration fluctuations in binary liquids.[16,17,32] Hence, from only the DLS data the most natural interpretation of the observed relaxation process is that it is caused by thermally driven long-range concentration fluctuations. However, previous studies of concentration fluctuations indicate that such a dynamical process should be associated with substantial structural inhomogeneities on a similar length scale,[33−36] which seems to be in conflict with our SANS data. The fact that the SANS measurements could not detect any significant small-angle scattering intensity in excess of a normal homogeneous liquid on length scales from 2 to 100 nm suggests that our ultraslow relaxation process has a different physical origin. In an attempt to understand the origin of our observed long-range diffusion process we have tried to estimate the hydrodynamic radius R_H of the self-diffusing particles by using the Stokes−Einstein relation,

$$D = \frac{k_B T}{6\pi R_H \eta_B} \quad (1)$$

where D is the diffusion constant of the particles undergoing Brownian motions, η_B is the viscosity of the Brownian medium, and R_H is the hydrodynamic radius of the diffusing particles. D is directly obtained from the $1/q^2$-dependent relaxation time τ, by the relation $D = 1/\tau q^2$, but it is less obvious what value should be used for the relevant "microscopic viscosity" η_B. In principle, two different approaches can be used. It can be assumed either that xylitol undergoes Brownian self-diffusion in a medium of water or that the diffusing xylitol particles feel the macroscopic viscosity of the solution. The first approach is probably giving a realistic value of the relevant viscosity at very high water concentrations and if the xylitol molecules would aggregate to large clusters, whereas the latter approach should be more realistic if the xylitol molecules are statistically distributed and diffusing individually. Since it is difficult to determine the most realistic approach without knowing the resulting hydrodynamic radius, we used both approaches, with the results presented in Figure 6. In Figure 6a the viscosity of bulk water has been used as the viscosity of the Brownian

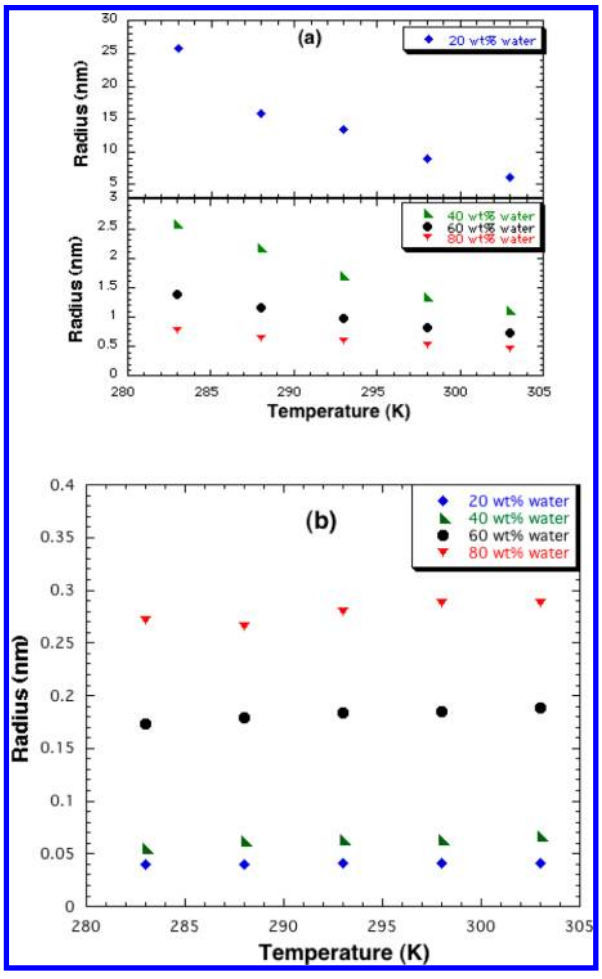

Figure 6. Using Stokes−Einstein relation the hydrodynamic radius of the long-range diffusing particles has been estimated from the measured diffusion constant of xylitol−water mixtures containing 20, 40, 60, and 80 wt % water. In (a) the viscosity of bulk water was used as the viscosity of the Brownian medium, and in (b) the macroscopic viscosity of each solution was used for the calculation.

dx.doi.org/10.1021/jp401633g | J. Phys. Chem. B 2013, 117, 7363−7369

medium, and despite the fact that this approach should underestimate the viscosity of the Brownian medium, particularly at low water concentrations and low temperatures, and thereby overestimating the size of the diffusing particles, the hydrodynamic radius becomes less than 2 nm at T = 293 K, except for the lowest water concentration of 20 wt %. However, at this lowest water concentration it cannot be realistic to use the viscosity of bulk water, particularly since no dramatic clustering of xylitol molecules seems to occur. Therefore, both these calculations as well as the SANS data are providing an upper size limit of possible xylitol clusters of 1−2 nm at $T \approx$ 293 K.

In Figure 6b we show the results obtained by using the macroscopic viscosity of each solution. It can be seen that particle size now becomes unrealistically small, i.e., smaller than the size of a xylitol molecule, particularly at low water concentrations, indicating that this approach overestimates the viscosity of the Brownian medium. In fact, the most correct viscosity to use is probably somewhere between the viscosity of bulk water and the bulk viscosity of the given solution. The conclusion of these calculations must therefore be that the xylitol molecules are self-diffusing as individual molecules or as small "clusters" of a few xylitol molecules (and perhaps some associated water molecules). This finding is in stark contrast to what was observed for aqueous solutions of glucose, maltose, and sucrose, where clusters of sugar molecules were rapidly growing with decreasing water content.[3] The question is, however, why no similar clusters are formed in xylitol−water solutions. Most likely, the answer can be found in the behavior of the hydrogen bonds in the different systems. In the case of xylitol it seems as if these molecules prefer to form hydrogen bonds to water molecules, rather than to other xylitol molecules, whereas the sugar molecules glucose, maltose, and sucrose prefer hydrogen bonding to other sugar molecules, thereby keeping water out from clusters of sugar molecules. Thus, xylitol appears to be more hydrophilic in character than these other sugar molecules. A more fundamental understanding of this is, however, still lacking.

The finding that no real clusters need to be formed in order to observe an ultraslow hydrodynamic relaxation process is an interesting observation, which makes it clear that one should be careful to interpret DLS processes with such characteristics as being caused by concentration fluctuations, provided that structural evidence are not also obtained.

In the q-range of the present DLS study it is evident that the relaxation time of the observed long-range diffusion process is several orders of magnitude longer than the relaxation time of the α-relaxation around room temperature. However, if its $1/q^2$-dependent relaxation time is extrapolated to q = 10 nm^{-1} the relaxation times of the two processes become similar. This q-value was chosen because it has been shown that it is possible to compare relaxation times measured by dielectric spectroscopy with those obtained by quasielastic neutron scattering at $q \approx$ 10 nm^{-1}.[37,38] In order to clarify this point we consider the Brownian motion of molecular/cluster units taking place in a viscous liquid and compare its characteristic time scale, τ, to the typical time scale of the structural relaxation, τ_α. Making use of the Stokes−Einstein relation to express the diffusion constant D and introducing the Maxwell's equation $\eta_B = G_\infty \tau_\alpha$, relating the viscosity η_B of the Brownian medium to its infinite-frequency shear modulus (or glass-modulus, G_∞) and to the structural relaxation time, one can formally derive a connection between the two time scales τ and τ_α:

$$\tau = \frac{6\pi R_H G_\infty}{q^2 k_B T}\tau_\alpha \quad (2)$$

In the same approximation used to estimate cluster-sizes in Figure 6b, i.e., assuming η_B as the macroscopic viscosity of the solution, τ_α would be an estimate for the dielectric α-process. Under these assumptions the two time scales would match for a particular value of the exchanged momentum

$$\bar{q} = \sqrt{\frac{6\pi R_H G_\infty}{k_B T}} \quad (3)$$

Due to the almost universal range of values of the unrelaxed shear modulus, $\bar{q}$ is generally not as dramatically system and temperature dependent as, for instance, the structural relaxation time is.

In the present case of water−xylitol mixtures, it is sufficient to assume a typical value for the glass-modulus $G_\infty \approx 10^8$−10^9 Pa (not strongly T-dependent) and a hydrodynamic radius in the range reported in Figure 6b, in order to obtain 5 nm^{-1} < $\bar{q}$ < 15 nm^{-1} even for a broad range of temperatures (200 K < T < 350 K). Furthermore, since the cooperative dielectric α-relaxation is expected to be q-independent at low momentum transfers, it would not be considerably longer if it was probed at a q-value similar to those of the present DLS study. Hence, it is only at low q-values that there is a large difference in time scale between the two relaxation processes around room temperature. This is most likely not a unique observation. Similar findings are expected for other types of solutions, where a process due to Brownian motion can be observed. The similar time scale of the two processes at high q-values further implies that the ultraslow Debye relaxation observed in dielectric studies of some hydrogen bonded liquids in general[5−9] and monoalcohols in particular[22,23,39−42] cannot be related to the here observed ultraslow DLS relaxation, which is best described as being caused by simple Brownian motion, as discussed above.

5. CONCLUSIONS

In this study we show that solutions of xylitol and water exhibit an ultraslow DLS relaxation due to long-range diffusion of single xylitol molecules or possibly small clusters of a few xylitol molecules and perhaps some associated water molecules. Thus, despite its similarities with previously observed concentration fluctuations in, e.g., sugar solutions, no significant clustering of the xylitol molecules can be observed. Rather, both the SANS and the DLS data indicate that the xylitol molecules are basically statistically dispersed in the solutions. The xylitol molecules undergo Brownian motions in the solutions and seem to feel a Brownian medium with a viscosity between that of bulk water and that of the given bulk solution.

Although the here observed DLS relaxation is considerably slower than the dielectrically observed α-relaxation around room temperature, its $1/q^2$-dependent relaxation time makes it about equally fast as the α-relaxation at an estimated q-value of dielectric spectroscopy. This further implies that our ultraslow DLS process cannot be related to the ultraslow Debye relaxation observed in dielectric studies of monoalcohols and some other hydrogen bonded liquids.

AUTHOR INFORMATION

Notes

The authors declare no competing financial interest.

■ ACKNOWLEDGMENTS

We thank David L. Sidebottom for valuable discussions. This work was financially supported by the Swedish Research Council and the Swedish Energy Agency. The Science & Technology Facilities Council and ISIS are thanked for the provision of neutron beam time.

■ REFERENCES

(1) Sidebottom, D. L. *Phys. Rev. E* **2007**, *76*, 011505.
(2) Patkowski, A.; Fischer, E. W.; Steffen, W.; Gläser, H.; Baumann, M.; Ruths, T.; Meier, G. *Phys. Rev. E* **2001**, *63*, 061503.
(3) Sidebottom, D. L. *Phys. Rev. E* **2010**, *82*, 051904.
(4) Patkowski, A.; Gläser, H.; Kanaya, T.; Fischer, E. W. *Phys. Rev. E* **2001**, *64*, 031503.
(5) Bergman, R.; Jansson, H.; Swenson, J. *J. Chem. Phys.* **2010**, *132*, 044504.
(6) Jansson, H.; Bergman, R.; Swenson, J. *Phys. Rev. Lett.* **2010**, *104*, 017802. Richert, R. *Phys. Rev. Lett.* **2010**, *104*, 249801. Jansson, H.; Bergman, R.; Swenson, J. *Phys. Rev. Lett.* **2010**, *104*, 249802.
(7) Yomogida, Y.; Minoguchi, A.; Nozaki, R. *Phys. Rev. E* **2006**, *73*, 041510.
(8) Kaminski, K.; Kaminska, E.; Adrjanowicz, K.; Wojnarowska, Z.; Wlodarczyk, P.; Grzybowska, K.; Dulski, M.; Wrzalik, R.; Paluch, M. *Phys. Chem. Chem. Phys.* **2010**, *12*, 723.
(9) Kaminski, K.; Kaminska, E.; Wlodarczyk, P.; Adrjanowicz, K.; Wojnarowska, Z.; Grzybowska, K.; Paluch, M. *J. Phys.: Condens. Matter* **2010**, *22*, 365103.
(10) Gallina, M. E.; Comez, L.; Perticaroli, S.; Morresi, A.; Cesàro, A.; De Giacomo, O.; Di Fonzo, S.; Gessini, A.; Masciovecchio, C.; Palmieri, L.; Paolantoni, M.; Sassi, P.; Scarponi, F.; Fioretto, D. *Philos. Mag.* **2008**, *88*, 3991.
(11) Patkowski, A.; Thurn, Th.; Banachowicz, E.; Steffen, W.; Bösecke, P.; Narayanan, T.; Fischer, E. W. *Phys. Rev. E* **2000**, *61*, 6909.
(12) Schramm, S.; Blochowicz, T.; Gouirand, E.; Wipf, R.; Stühn, B.; Chushkin, Y. *J. Chem. Phys.* **2010**, *132*, 224505.
(13) Fischer, E. W.; Becker, Ch.; Hagenah, I.-U.; Meier, G. *Prog. Colloid Polym. Sci.* **1989**, *80*, 198.
(14) Patkowski, A.; Fischer, E. W.; Meier, G.; Nilgens, H.; Steffen, W. *Prog. Colloid Polym. Sci.* **1993**, *91*, 35.
(15) Fischer, E. W. *Phys. A* **1993**, *201*, 183.
(16) Fischer, E. W.; Bakai, A. *J. Chem. Phys.* **2004**, *120*, 5235.
(17) Kanaya, T.; Patkowski, A.; Fischer, E. W.; Seils, J.; Glaser, H.; Kaji, K. *Acta Polym.* **1994**, *45*, 137.
(18) Kanaya, T.; Patkowski, A.; Fischer, E. W.; Seils, J.; Glaser, H.; Kaji, K. *Macromolecules* **1995**, *28*, 7831; *Chem. Phys.* **2010**, *132*, 224505.
(19) Vogel, H. *Phys. Z.* **1921**, *22*, 645.
(20) Fulcher, G. S. *J. Am. Ceram. Soc.* **1925**, *8*, 339.
(21) Tammann, G.; Hesse, W. *Z. Anorg. Allg. Chem.* **1926**, *156*, 245.
(22) Jansson, H.; Swenson, J. *J. Chem. Phys.* **2011**, *134*, 104504.
(23) Gainaru, C.; Schildmann, S.; Böhmer, R. *J. Chem. Phys.* **2011**, *135*, 174510.
(24) Elamin, K.; Sjöström, J.; Jansson, H.; Swenson, J. *J. Chem. Phys.* **2012**, *136*, 104508.
(25) Inaba, A.; Andersson, O. *Thermochim. Acta* **2007**, *461*, 44.
(26) Hayashi, Y.; Puzenko, A.; Feldman, Y. *J. Non-Cryst. Solids* **2006**, *352*, 4696.
(27) Berne, B. J.; Pecora, R. *Dynamic Light Scattering*; Wiley: New York, 1976.
(28) http://www.isis.stfc.ac.uk/ (accessed Feb 2013).
(29) Heenan, R. K.; King, S. M.; Turner, D. S.; Treadgold, J. R. *Proc ICANS-XVII* **2006**, 780−785.
(30) http://www.mantidproject.org (accessed Feb 2013).
(31) Swenson, J.; Elamin, K.; Jansson, H.; Kittaka, S. *Chem. Phys.* **2012**, DOI: 10.1016/j.chemphys.2012.11.014.
(32) Gerharz, B.; Meier, G.; Fischer, E. W. *J. Chem. Phys.* **1990**, *92*, 7110.
(33) Silescu, H. *J. Non-Cryst. Solids.* **1999**, *243*, 81.
(34) Böhmer, R. *Curr. Opin. Solid State Mater. Sci.* **1998**, *3*, 378.
(35) Angell, C. A.; Ngai, K. L.; McKenna, G. B.; McMillan, P. F.; Martin, S. W. *J. Appl. Phys.* **2000**, *88*, 3113.
(36) Ngai, K. L. *J. Non-Cryst. Solids* **2000**, *275*, 7.
(37) Arbe, A.; Alegria, A.; Colmenero, J.; Hoffmann, S.; Willner, L.; Richter, D. *Macromolecules* **1999**, *32*, 7572.
(38) Swenson, J.; Schwartz, G. A.; Bergman, R.; Howells, W. S. *Eur. Phys. J. E* **2003**, *12*, 179.
(39) Wang, L.; Richert, R. *J. Phys. Chem. B* **2005**, *109*, 11091.
(40) Hansen, C.; Stickel, F.; Berger, T.; Richert, R.; Fischer, E. W. *J. Chem. Phys.* **1997**, *107*, 1086.
(41) El Goresy, T.; Böhmer, R. *J. Chem. Phys.* **2008**, *128*, 154520/1.
(42) Jakobsen, B.; Maggi, C.; Christensen, T.; Dyre, J. C. *J. Chem. Phys.* **2008**, *129*, 184502.